NAVAL POSTGRADUATE SCHOOL
Monterey, California

UNITED STATES NAVY
· NAVAL POSTGRADUATE SCHOOL ·

DTIC
S ELECTE D
E
MAY 28 1993

THESIS

EXERGY DECREASE IN SHOCK WAVES
AND BOUNDARY LAYERS
OF SPACE LAUNCH VEHICLES

by

Benjamin F. Roper

MARCH, 1993

Thesis Advisor: C. F. Newberry

93 6 00 054

93-12545

REPORT DOCUMENTATION PAGE

1a Report Security Classification: Unclassified			1b Restrictive Markings			
2a Security Classification Authority			3 Distribution/Availability of Report			
2b Declassification/Downgrading Schedule			Approved for public release; distribution is unlimited.			
4 Performing Organization Report Number(s)			5 Monitoring Organization Report Number(s)			
6a Name of Performing Organization Naval Postgraduate School		6b Office Symbol (if applicable) AE	7a Name of Monitoring Organization Naval Postgraduate School			
6c Address (city, state, and ZIP code) Monterey CA 93943-5000			7b Address (city, state, and ZIP code) Monterey CA 93943-5000			
8a Name of Funding/Sponsoring Organization		6b Office Symbol (if applicable)	9 Procurement Instrument Identification Number			
Address (city, state, and ZIP code)			10 Source of Funding Numbers			
			Program Element No	Project No	Task No	Work Unit Accession No
11 Title (include security classification) EXERGY DECREASE IN SHOCK WAVES AND BOUNDARY LAYERS OF SPACE LAUNCH VEHICLES						
12 Personal Author(s) ROPER, Benjamin Frank						
13a Type of Report Master's Thesis		13b Time Covered From To	14 Date of Report (year, month, day) 1993 March 25		15 Page Count 59	
16 Supplementary Notation The views expressed in this thesis are those of the author and do not reflect the official policy or position of the Department of Defense or the U.S. Government.						

17 Cosati Codes			18 Subject Terms (continue on reverse if necessary and identify by block number)
Field	Group	Subgroup	exergy;entropy;space launch vehicles;exergy method of analysis:shock waves;boundary layers

19 Abstract (continue on reverse if necessary and identify by block number)
The exergy method of analysis uses both the First and Second laws of Thermodynamics to determine where losses occur. This method has been shown to be superior to conventional heat balance analyzes. A primary contributor to the exergy decrease is the production of entropy. Entropy is produced in shock waves and boundary layers, as well as in other regions of the flowfield. A method of analysis is presented to quantify the entropy that is produced in the bow shock wave and the boundary layer of a space launch vehicle for Mach numbers between 1.1 and 10.

20 Distribution/Availability of Abstract X unclassified/unlimited __ same as report __ DTIC users	21 Abstract Security Classification Unclassified	
22a Name of Responsible Individual NEWBERRY, Conrad	22b Telephone (include Area Code) (408)656-2311	22c Office Symbol AA/NE

DD FORM 1473, 84 MAR   83 APR edition may be used until exhausted   security classification of this page

All other editions are obsolete   Unclassified

i

Exergy Decrease in Shock Waves and Boundary Layers
of Space Launch Vehicles

by

Benjamin F. Roper
Lieutenant Commander, United States Navy
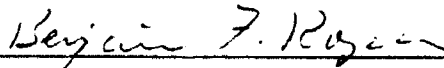B.S., Stephen F. Austin State University, 1977

Submitted in partial fulfillment
of the requirements for the degrees of

MASTER OF SCIENCE IN SYSTEMS TECHNOLOGY (SPACE SYSTEMS OPERATIONS)
and
MASTER OF SCIENCE IN ENGINEERING SCIENCE

from the

NAVAL POSTGRADUATE SCHOOL
March 1993

Author: _____

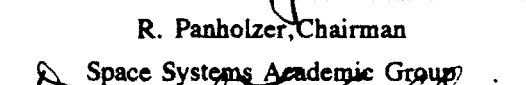Benjamin F. Roper

Approved by: _____

C. F. Newberry, Thesis Advisor

_____

D. W. Netzer, Second Reader

_____

R. Panholzer, Chairman

Space Systems Academic Group

_____

Daniel J. Collins, Chairman, Department of Aeronautics
and Astronautics

ii

ABSTRACT

The exergy method of systems analysis uses both the First and Second laws of Thermodynamics to determine where losses occur. This method has been shown to be superior to conventional heat balance analyzes. A primary contributor to the exergy decrease is the production of entropy. Entropy is produced in shock waves and boundary layers, as well as in other regions of the flowfield. A method of analysis is presented to quantify the entropy that is produced in the bow shock wave and the boundary layer of a space launch vehicle for Mach numbers between 1.1 and 10.

Accesion For		
NTIS CRA&I		☒
DTIC TAB		☐
Unannounced		☐
Justification		
By		
Distribution /		
Availability Codes		
Dist	Avail and / or Special	
A-1		

DTIC QUALITY INSPECTED 2

TABLE OF CONTENTS

ACKNOWLEDGEMENTS

The author wishes to extend his heartfelt thanks to the following people whose guidance and support made this paper possible:

Dr. D.W. Netzer whose suggestions and advice were instrumental in providing a better paper;

Dr. C.F. Newberry who was never too busy to explain a particular point, even for the third or fourth time, and who deserves more than a little of the credit for the completion of this work.

Finally, the author recognizes Patricia Roper for her continued support and encouragement.

LIST OF SYMBOLS

Symbol	Description	Units
A	Area	m^2
A_1	The angle the flow must turn through in traveling from the sonic line to the cone of the body	deg.
C	Shape factor for the nose of the body used in determining shock detachment distance	
C_{pmax}	Maximum value of the pressure coefficient	
c_p	Specific heat at constant pressure	$J/(kg\text{-}K)$
c_v	Specific heat at constant volume	$J/(kg\text{-}K)$
D	Drag	N
D'	Twice the nose radius	m
d'	Diameter or height in plane of point on body determined by angle for shock detachment	m
E	Emissive power	W/m^2
e	Internal energy, per unit mass	J/kg
F	Shape factor, used in radient energy calculations	
F'	Horizontal distance measured from center of curvature of the nose to point on shock	m
g	Local acceleration due to gravity	m/s^2
g_c	Constant in Newton's law	$\dfrac{(kg\text{-}m)}{(N\text{-}s^2)}$
h	Enthalpy, per unit mass	J/kg
J	Joules	$kg\text{-}m^2/s^2$
J'	Joule's constant (ft-lbs mechanical energy per Btu of heat)	
M	Mach number	
M_f	Freestream Mach number at the edge of the wake	
M_w	Minimum Mach number of the flow in the wake, located at the center of the wake	
N	Number of species	
p	Pressure	N/m^2
q	Dynamic pressure	N/m^2
Re	Reynolds number	
Re_T	Transition Reynolds number	

Re_x	Reynolds number as a function of body length	
R	Nose Radius	m
R'	Specific gas constant	J/(kg-K)
R_b	Radius of the base of the body	m
r	Radius of the wake at the profile calculation point	m
S	Entropy	J
s	Entropy, per unit mass	J/kg
SPA	Angle between the body center-line and the sonic point on the body	deg.
T	Temperature	K
U	Freestream velocity	m/s
U_w	Minimum velocity in the wake	m/s
u	Local velocity	m/s
V	Magnitude of the velocity gradient at the stagnation point	
v	Volume	m^3
x	Horizontal ordinate (freestream direction)	m
x'	Horizontal distance from most forward point on shock to plane containing d'	m
x_o	Distance from the most forward point of detached shock to intercept of its asymptote on x-axis	m
y	Vertical ordinate (normal to freestream direction)	m
z	altitude	m

Greek

β	$(M^2 - 1)^{1/2}$	
δ	Boundary layer thickness	m
δ_t	Calculated boundary layer thickness extended to the point in the wake where the velocity profile is calculated	m
δ_{det}	Deflection angle for shock wave detachment of a conical body	deg.
γ	Ratio of specific heats	
η	Angle between normal to free-stream direction and sonic line	deg.
ρ	Density	kg/m^3
θ	Shock wave angle w.r.t. free-stream	deg.
θ_1	Angle between freestream and a line tangent to the body surface	deg.

μ	Coefficient of viscosity	kg/m-s
μ_∞	Freestream Mach angle	deg.
ν	Prandtl-Meyer function	

Subscripts

0	Indicates stagnation condition
1	Freestream condition
2	Condition immediately behind the shock wave
e	Condition at the boundary layer edge
o	Reference condition

I. INTRODUCTION

As commercial interest in space launch vehicles has increased over the last twenty years, there has been an increased emphasis on improving the efficiency of vehicles used for space launch services. This emphasis will continue to receive attention as competition forces the providers of launch services to decrease costs.

This thesis is an initial step in the development of an exergy methodology tool for the conceptual, preliminary, and detailed design of aerospace vehicles.

In order to determine the efficiency of a particular launch system, it is necessary to identify the various sources of efficiency loss and the quantity of efficiency loss associated with each source within the system. Although energy cannot be created or destroyed, it can be transformed into unavailable forms. This thesis will present an investigation of one method that may be used to examine the efficiency loss from two specific areas of a typical launch vehicle. This method uses the concept of available energy or exergy as the basis for determining the decrease in the energy state that occurs in the shock wave and the boundary layer of a supersonic vehicle.

Typical performance analyzes of energy systems use only the first law of thermodynamics. This method of analysis is

1

based on the principle of conservation of energy, and suggests that an energy balance accounting for all energy flow into or out of the system will provide a measure of the system efficiency. While the first law approach is extremely important in the performance analysis of energy systems, it provides only the overall performance or the actual gross performance of the system or process. To establish the magnitude, location, and type of loss within a system it is necessary to use the Second law of Thermodynamics. The second law accounts for the irreversibility of all real processes and thus provides a method of calculating the losses associated with entropy production that occurs.

The exergy method of analysis uses both the First and Second laws of Thermodynamics to determine the energy that is available at various points in a system. While the exergy method of analysis has been applied to conventional closed cycle thermal systems such as power generation and refrigeration systems, it has not, to the author's knowledge, been applied to the open cycle space launch vehicle.

"Exergy is defined as the work that is available in a gas, fluid, or mass as a result of its nonequilibrium condition relative to some reference condition."[Ref. 1:p. 33] Since exergy is defined as the available work in a gas, fluid, or mass, it is a special case of defining available

energy. Exergy is an explicit property, and therefore can be calculated at any point in an energy system.

The exergy method permits the examination of any process in relation to the theoretically most efficient manner that the process could be carried out within the environment. An exergy analysis allows one to quantify the loss of efficiency in a process due to the loss of the quality of the energy.

Exergy is calculated relative to a reference condition by the following general equation:[Ref. 1:p. 34]

$$Exergy = (u - u_o) - T_o(s - s_o) + \frac{P_o}{J}(v - v_o) + \frac{V^2}{2gJ} +$$
$$(z - z_o)\frac{J}{g_c J} + \sum_{0}^{c}(\mu_c - \mu_o)N_c + \qquad (1)$$
$$E_i A_i F_i (3T^4 - T_o^4 - 4T_o T_3) + \ldots$$

where the subscript o denotes the reference condition. The terms on the right side of the equation are internal energy, change in heat energy, flow work, kinetic energy per unit mass, potential energy, chemical energy, and radiation energy emission respectively. In the analysis of specific systems or processes one or more of the above terms may be omitted, and only those relevant to the problem being considered need be included.[Ref 1:pp.34-36]

This thesis focuses on the quantity of exergy decrease as a result of entropy production across the shock wave and as a result of boundary layer formation. As can be seen from equation 1, an increase in entropy results in a decrease in

3

exergy. The Second law of Thermodynamics tells us that all real process are irreversible and that entropy is increased in an irreversible process.

II. EXERGY DECREASE ACROSS THE SHOCK WAVE

Supersonic flow over a blunt body will result in the bow shock wave being detached from the body as shown in Figure 1. The shape of the detached shock wave, its detachment distance, and the flowfield between the body and the shock are determined by the shape of the body and the free stream Mach number. [Ref.2:p.128-129]
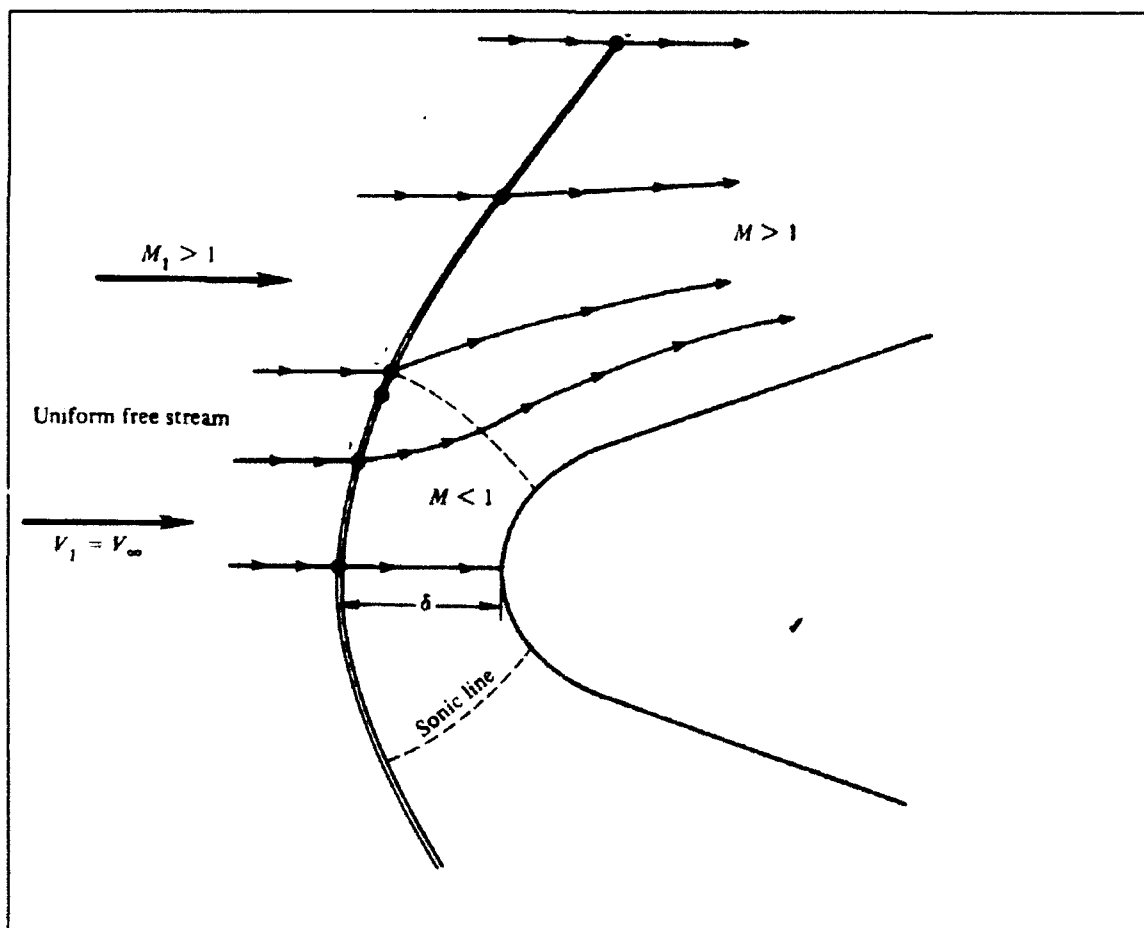

Figure 1: Supersonic Blunt Body in Flowfield.

Since the velocity of the body is supersonic, the flow ahead of the body is unaware of the presence of the body until the shock wave is encountered. The shock wave directly in front of the body is approximately normal to the free stream and consequently the flow behind the shock wave at this point is subsonic. The subsonic flow region is defined by the shock wave, the body, and the sonic line as shown in Figure 1.

Because the flowfield between a blunt body and its detached shock wave contains both subsonic and supersonic flow, an exact determination of the flowfield dynamics is extremely complicated to formulate. The steady state flowfield in the subsonic region is described by elliptic equations and in the supersonic region by hyperbolic equations. The sonic line divides these two regions. It is the problem of predicting the flowfield in the transition region between the subsonic and supersonic flow that makes the flowfield calculations for a supersonic blunt body so difficult.

The flowfield behind a detached shock wave cannot be precisely determined without the application of sophisticated numerical methods. In keeping with the development of a design tool, a simplified method for determining the approximate shape of the detached shock wave that was developed by Moeckel [Ref. 3] is used. This method was subsequently examined by Love [Ref. 4] and with some

modification was found to be valid for blunt bodies traveling at supersonic and hypersonic speeds.

Love introduced two major modifications to Moeckel's method. The first of these was in the method used to calculate the shock detachment distance from the body. Moeckel used a continuity relation to calculate detachment distance and shock shape. Love calculates shock detachment distance by the following equation:

$$\frac{x^{\prime}}{d^{\prime}} = 0.5 C \cot \delta_{det} \qquad (2)$$

where x'/d' is the nondimensional detachment distance, C is a factor that depends on type of body (spherical, cylindrical, etc.), and δ_{det} is the required deflection angle for shock wave detachment, from a conical body, for the given Mach number (see Figure 2).

The second modification made by Love was in the calculation of the angle eta (η) that the sonic line makes with the freestream. Love conducted wind tunnel tests and compared his experimental results with his theoretical calculations [Ref.4:pp.13-15]. For this analysis, the angle η corresponding to 1.1≤M≤10 was obtained by developing the following analytical expression for the values of η vs Mach number as set forth by Love [Ref.4:p.45]:

$$\eta = \frac{3.9901 + 56.9298 * log(M)}{57.29578} \qquad (3)$$
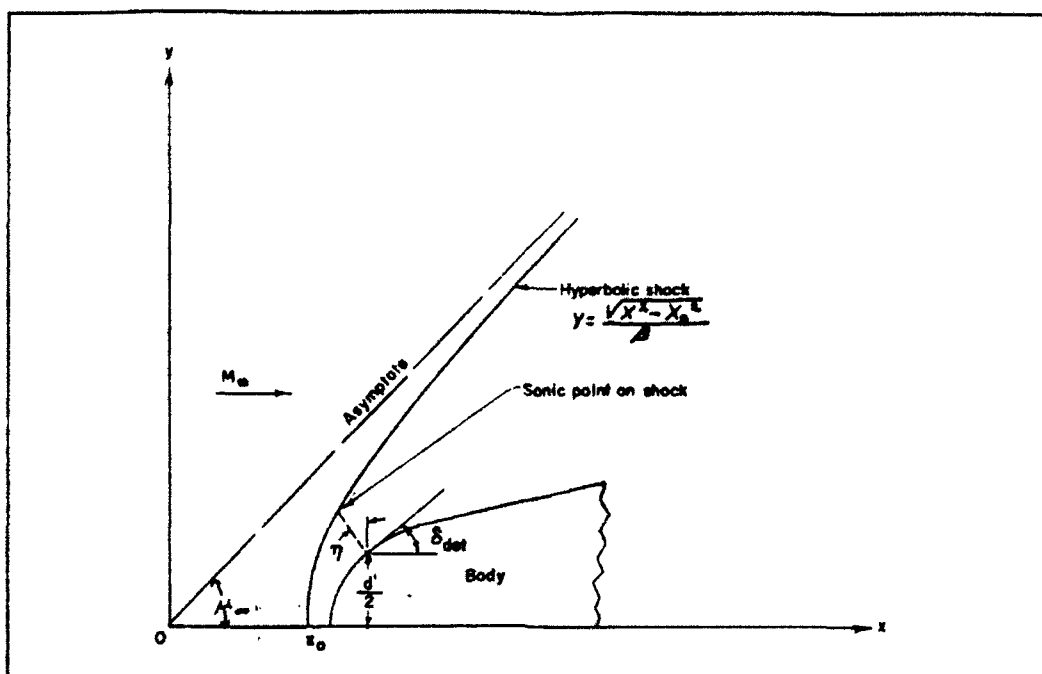
Figure 2: Representation of Flow With Detached Shock and Notation Used in Analysis.

A. BODY SHAPE

The shape of the deflecting body is one of the factors determining the shock wave shape. For this study, the body was patterned somewhat loosely after the Titan III-A launch vehicle. This body shape is essentially a blunt cone and cylinder arrangement. The dimensions of the launch vehicle used in the analysis are shown in Table 1.

TABLE 1: LAUNCH VEHICLE DIMENSIONS

Length Overall	120 Ft.
Diameter	10 Ft.
Nose Radius	1.5 Ft.
Nose Cone Length	10 Ft.

B. MACH NUMBER

Besides the shape of the body, the other factor in determining the shape of the shock wave is the freestream Mach number. This study determined the shock shape based on $1.1 \leq M \leq 10$. Although this is far short of the Mach number required to reach orbit, the purpose of the study was to demonstrate the validity of the method, which can be accomplished in the listed Mach range.

C. ASSUMPTIONS

The method of approximating the shock shape and location developed by Moeckel is based on two assumptions:

(1) The form of the shock between its foremost point and its sonic point is adequately represented by a hyperbola asymptotic to the free stream Mach lines; and
(2) the sonic line between the shock and body is straight and inclined at an angle that depends only on the freestream Mach number. [Ref.3:p.1]

The first assumption states that the shock shape between its vertex, or foremost point, and its sonic point may be represented by a hyperbola. For this study, the assumption was made that this approximation for the shock shape is valid past the sonic point of the shock wave. For calculation purposes, the shock wave was taken from the vertex of the wave to the point where the angle between the shock wave and the asymptote that defines the hyperbola differ by no more than one per cent. The equation for the hyperbola used in these assumptions is

$$y = \frac{\sqrt{x^2 - x_o^2}}{\beta} \qquad (4)$$

where x is the longitudinal axis of the body, y is the axis perpendicular to the x axis, β is the cotangent of the Mach angle, and x_o is the distance from the vertex of the shock wave to the intersection of its asymptotes.[Ref.3:p.1]

The second assumption made by Moeckel concerning the sonic line was modified by Love as previously discussed and was used in this analyzes.

Air is the fluid used for all of the analysis presented in this thesis. However, the analysis method is equally valid for any gas, and would only require using the appropriate value for the ratio of specific heats (γ) and the new specific gas constant. It has been assumed that the fluid behaves as a perfect gas in all of the calculations. This assumption is valid for velocities up to approximately M=3 to M=5 [Ref 5:pp.17-20]. Above these velocities dissociation of the fluid begins to occur due to atmospheric heating. If the gas continues to be heated, ionization will occur. As the degree of dissociation and ionization increases, the perfect gas assumption becomes less valid.

The calculation of total entropy across the shock wave requires a determination of the mass flow rate of air through the shock wave. The air mass flow rate calculation is based on the density, cross sectional area being studied, and the velocity of the air. Since the density of air in the

10

atmosphere varies with height above sea level, an arbitrary height of 30,000 meters was assumed for all M values. The density and temperature of air at this altitude was taken from the International Civil Aviation Organization (ICAO) standard atmosphere tables [Ref 6]. The calculations may be used for any altitude by inserting the appropriate density and temperature.

D. EXERGY CALCULATION

From equation (1), and neglecting all terms on the right except the entropy term, the total exergy decrease through the shock wave is proportional to the increase in entropy across the shock. The entropy change across a shock is given by [Ref. 7:p. 10)

$$\frac{\Delta s}{c_v} = \ln(\frac{2\gamma M_1^2 \sin^2\theta - (\gamma-1)}{\gamma+1}) - \gamma\ln(\frac{(\gamma+1)M_1^2\sin^2\theta}{(\gamma-1)M_1^2\sin^2\theta+2}) \quad (5)$$

where c_v is the specific heat at constant volume for air, γ is the ratio of specific heats, M is the freestream Mach number, and θ is the local shock wave angle with reference to the freestream direction. By using the method of Moeckel, modified by Love, to determine the approximate shock shape, the entropy increase across the total shock was calculated by equation 5 and numerical integration using cumulative applications of Simpson's Rule. The number of integrations varied with the shock strength and shape running from a low of 50 for Mach=1.1 to a high of 2513 for Mach=10.

11

The entropy calculations were performed by the Fortran 77 program contained in Appendix A. For the assumed body shape, this program calculates the approximate shock wave shape and the total rate of entropy change across the shock for a designated control volume and designated Mach numbers between 1.1 and 10. The calculations are carried to three decimal places with the knowledge that assumptions and round-off error may have affected the accuracy. The results are summarized in Table 2.

TABLE 2: ENTROPY CHANGE ACROSS SHOCK

Mach Number	Rate of Entropy Change Across Shock (KJ/sec)
1.1	. . 9
2.0	50.803
3.0	301.469
4.0	836.941
5.0	1662.150
6.0	2764.771
7.0	4131.494
8.0	5759.238
9.0	7641.229
10.0	9774.107

As can be seen from equation 5, the entropy rise across the shock increases as the shock wave angle (θ), and the freestream Mach number (M_1) increase. For a detached shock wave, the shock wave angle is greatest immediately ahead of the body where it is approximately normal to the freestream and decreases as it curves around the body until it

eventually asymptotes the freestream. This indicates that
for a given body shape and Mach number, the greatest exergy
loss occurs in the vicinity of the vertex of the shock wave.
This is shown graphically in Figure 3. The vertical axis is
shown as entropy change over the specific gas constant (R′),
and the horizontal axis is shown as the angle phi (ϕ), which
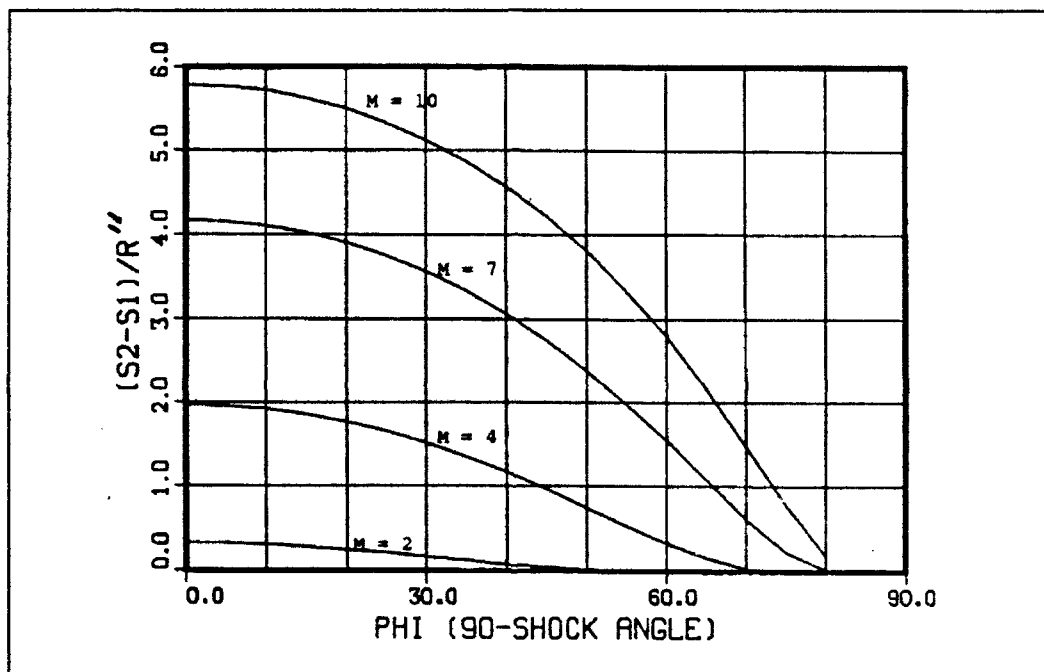is 90 - θ.

Figure 3: Entropy Rise Across Shock Wave.

E. VERIFICATION OF THE COMPUTER MODEL

Comparisons between theoretical shock location using the
program of Appendix A and actual shock location as
determined by Love for Mach numbers of 1.94 and 6.8 for a
combination sphere and cylinder body shape are shown in
Figures 4 and 5 respectively. These comparisons show good

agreement between calculated shock shape and shock location. The data points corresponding to experimental results were taken from charts [Ref. 4:pp 46,51] and therefore, precise quantitative evaluations regarding goodness of fit are not possible. However, the experimental data appear to be within five percent of the predicted values of the shock profile.
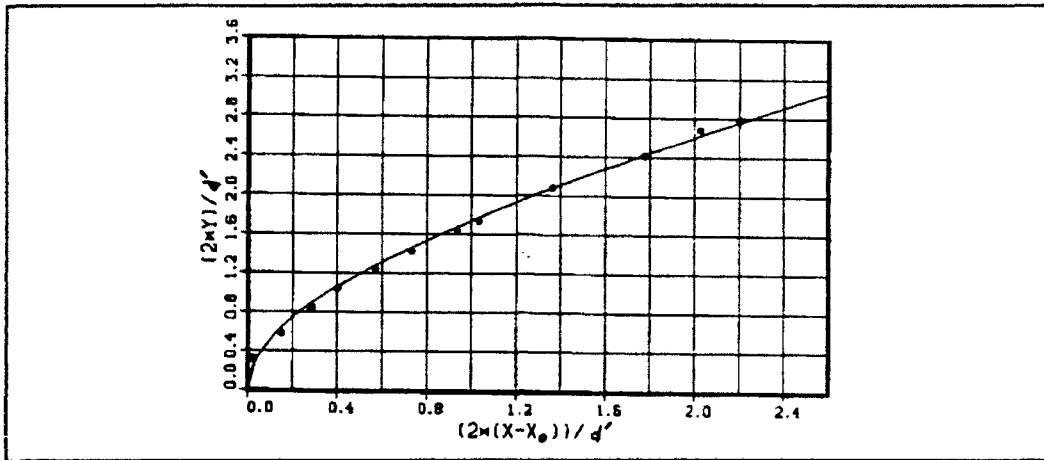
Figure 4: Comparison of Experimental and Predicted Shock Shape. Mach 1.94
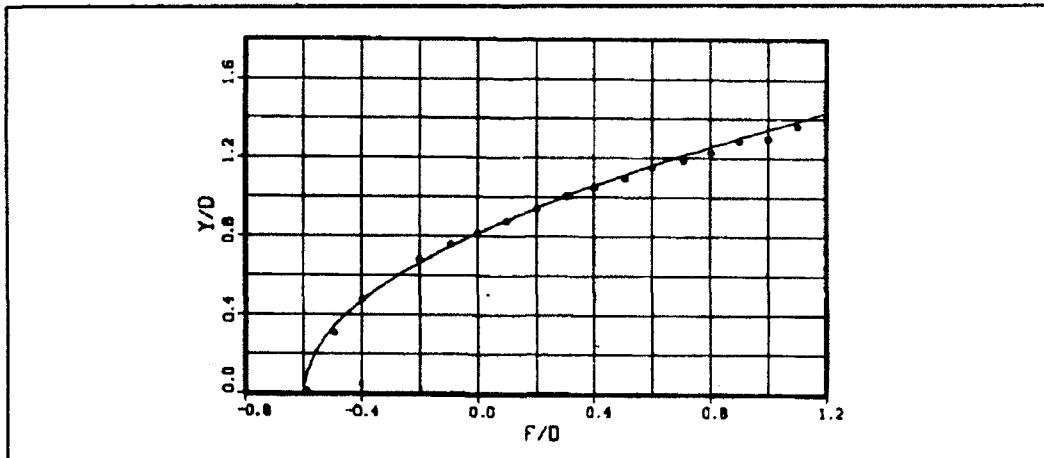
Figure 5: Comparison of Experimental and Predicted Shock Shape. Mach 6.8

14

Another reality check for the computer model was made by calculating the mass flow of air through the control volume defined by the shock wave at $1.1 \leq M \leq 10$ at an altitude of 30,000 meters. Since the vehicle is supersonic, there is no deflection of the flow around the body prior to passing through the shock. The validity of the shock shape generated by the program is good as shown in Figures 4 and 5 above. The shock wave may be thought of as a blunt cone. If the cone is terminated at any point, the distance from the centerline to the shock is the radius of the base. The mass flow through the area of the base can be easily calculated. This was done and the result was compared with the mass flow calculated by the program using the same Simpson's rule integration technique that was used to calculate the entropy rise across the shock. The results of these two calculations differed by less than three per cent for all Mach numbers.

III. EXERGY DECREASE IN THE BOUNDARY LAYER

If a control volume is taken around a cylindrical body moving through a gas, there will be a change in the momentum of the gas taken upstream of the body from that taken downstream of the body. This difference in momentum is a function of the drag on the body, and is given by [Ref. 8:pp. 23-24]

$$D = \int_A \rho \, u \, (U-u) \, dA \qquad (6)$$

where the integral is taken over the end surface of the cylinder at a large distance downstream, U is the velocity upstream, and u is the velocity at an arbitrary point in the wake. Letting

$$U-u = -\int_0^\infty (\frac{\partial u}{\partial y} dy + \frac{\partial u}{\partial z} dz) \qquad (7)$$

According to Crocco's theorem [Ref. 9]

$$-(\frac{\partial u}{\partial y} dy + \frac{\partial u}{\partial z} dz) = \frac{T}{u}(\frac{\partial s}{\partial y} dy + \frac{\partial s}{\partial z} dz) \qquad (8)$$

Substituting equations 7 and 8 into equation 6, we get

$$D = \int_A \rho u dA \int_0^\infty \frac{T}{u}(\frac{\partial s}{\partial y} dy + \frac{\partial s}{\partial z} dz) \qquad (9)$$

Replacing $\rho u dA$ (the mass flow through the cross-sectional area dA) by dm and T/u by T_∞/U, which is justified if second order terms are neglected [Ref. 8:p.24], in equation 9 gives

$$D = \frac{T_\infty}{U} \int_A dm(s - s_\infty) \qquad (10)$$

Taking the integral over the area of the wake, equation 10 can be written as

$$DU = T_\infty \frac{S}{\sec} \qquad (11)$$

This is an application of the theory of Oswatitsch [Ref. 10]. The freestream temperature and velocity are known or can be calculated using the ICAO tables [Ref. 6] for a given altitude and Mach number. If the drag can be calculated, then the entropy increase can be calculated using equation 11. To calculate the profile drag of the body, the flow parameters at the boundary layer edge and the boundary layer shape are needed.

The theory that the flow surrounding an immersed body could be divided into two parts was first proposed by L. Prandtl in 1904. Prandtl stated that the viscosity in the major part of the flow field has a negligible effect on its motion and consequently in most cases could be ignored. The other part of the flow field consisted of a narrow region next to the body where the viscous forces are not negligible. [Ref.11]

This narrow region near the body is known as the boundary layer. In the boundary layer the velocity of the fluid increases rapidly from zero at the surface to a value which then changes slowly with increasing distance from the

17

body. At an infinite distance from the body, the boundary
layer and the freestream merge smoothly together. For
practical applications, the boundary layer conditions
approach the freestream condition very rapidly within a
relatively small distance from the surface as shown in
Figure 5.
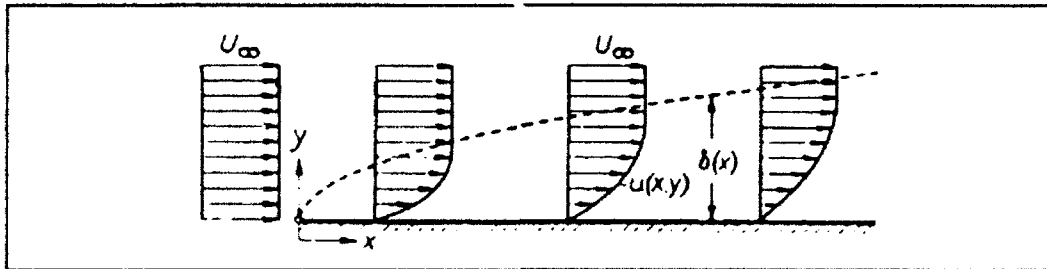
Figure 6: Boundary Layer on a Flat Plate [Ref. 10:p. 25]

If the freestream velocity is taken as U, then the edge of
the boundary layer may be designated as that distance from
the body where the velocity of the stream is .995U or u_e.

Boundary layers may be either laminar or turbulent. In
laminar flow, the flow within the boundary layer is
characterized by smooth streamlines approximately parallel
to the surface and there is little mixing. In the turbulent
boundary layer the flow experiences irregular fluctuations
in velocity magnitude and direction superimposed on the mean
flow, which remains roughly parallel to the surface
[Ref. 12:p.11].

The change from laminar to turbulent flow is referred to
as transition. Transition may be caused by a number of

18

factors including disturbances that occur in the freestream, surface roughness, changes in the pressure distribution on the surface of the body, or an increase in Reynolds number. Reynolds number is a ratio of the inertia to viscous forces in a fluid and is given by the following equation:

$$Re = \frac{U\rho l}{\mu} \qquad (12)$$

where U is the velocity, ρ is the density, l is the body dimension, and μ is the dynamic coefficient of viscosity of the fluid.

The presence of shear forces in the boundary layer due to friction and the viscous nature of the fluid result in heat being generated. The heat is transferred to the body and to the fluid. The viscous dissipation as heat in the boundary layer results in an increase in entropy and consequently a decrease in exergy. At hypersonic velocities, the intense viscous dissipation may result in temperatures high enough to cause dissociation and ionization of the surrounding air [Ref. 5:p. 228]. This phenomenon and its effects will not be discussed in this paper. However, the error introduced by ignoring these effects can be significant. Interpolating from Anderson [Ref. 5:p. 511], the error, at M=10 and at 30,000 meters, in the ratio T_2/T_1 across a normal shock is approximately 24 per cent.

A. BOUNDARY LAYER CALCULATIONS

An exact determination of the flow conditions in and surrounding the boundary layer for a body of arbitrary shape is possible by solving the three dimensional Navier-Stokes equations. These equations do not have a closed form solution, but require elaborate computer methods to be solved. However, if we specify that the boundary layer thickness (δ) is much less than the length of the body, and that the Reynolds number is large ($>10^5$), the Navier-Stokes equations can be reduced to the boundary layer equations:

$$\text{Continuity:} \quad \frac{\partial(\rho u)}{\partial x} + \frac{\partial(\rho v)}{\partial y} = 0 \tag{13}$$

$$x\ Momentum: \quad \rho u \frac{\partial u}{\partial x} + \rho v \frac{\partial u}{\partial y} = -\frac{dp_e}{dx} + \frac{\partial}{\partial y}\left(\mu \frac{\partial u}{\partial y}\right) \tag{14}$$

$$y\ Momentum: \quad \frac{\partial p}{\partial y} = 0 \tag{15}$$

$$Energy: \quad \rho u \frac{\partial h}{\partial x} + \rho v \frac{\partial h}{\partial y} = \frac{\partial}{\partial y}\left(k \frac{\partial T}{\partial y}\right) + u \frac{dp_e}{dx} + \mu \left(\frac{\partial u}{\partial y}\right)^2 \tag{16}$$

where x is the direction parallel to the surface, y is the direction normal to the surface, u is the velocity component in the x direction, v is the velocity component in the y direction, ρ is the density, p_e is the pressure at the outer edge of the boundary layer, μ is the viscosity coefficient of the fluid, h is the enthalpy, and k is the thermal conductivity of the fluid.

Like the Navier-Stokes equations, the boundary layer
equations are nonlinear. They are simpler and easier to
solve, but still require computer methods to obtain exact
solutions in most cases. Solution methods for the boundary
layer equations are presented by Young [Ref. 12] and
Schlichting [Ref. 14].

1. Approximate Methods

The purpose of this thesis was not to determine an
exact solution to the boundary layer equations, but to show
that an exergy analysis can be conducted on the boundary
layer and to provide the foundation for an exergy based
design tool and or methodology. This concept can be
demonstrated by making several approximations that will
provide rough estimates of the required variables without
the extensive numerical and computer calculations required
to obtain a more exact solution of the boundary layer
equations. The necessary calculations are developed in the
following paragraphs.

a. *Stagnation Point Calculation*

As stated in the preceding chapter, the flow
field surrounding a blunt body traveling at supersonic
velocity will consist of both subsonic and supersonic flow
divided by the sonic line (see Figure 1). For a body at zero
angle of attack, the flow precisely along the body axis will
pass through the shock wave, which at that point is normal
or very nearly normal to the freestream direction, slow, and

21

stop at the stagnation point. On a blunt body, the boundary layer has a finite thickness at the stagnation point. The boundary layer thickness at the stagnation point of a two dimensional body is given by

$$\delta(0) = \sqrt{\frac{0.075\mu}{\rho V}} \qquad (17)$$

where $\delta(0)$ is the boundary layer thickness at the stagnation point, and V is the magnitude of the velocity gradient at the stagnation point. [Ref. 15:pp. 208-209]

The velocity gradient is determined by the method of Anderson [Ref. 5:pp. 255-256]. It can be shown using Euler's equation applied at the boundary layer that,

$$\frac{du_e}{dx} = -\frac{1}{\rho_e u_e}\frac{dp_e}{dx} \qquad (18)$$

where the subscript e indicates conditions at the edge of the boundary layer, u is the velocity component in the x direction which is parallel to the body, and p is the pressure. Assuming a modified newtonian pressure distribution over the surface, the pressure coefficient is given by [Ref. 5:p. 53]

$$C_p = C_{P_{max}}\sin^2\theta_1 \qquad (19)$$

where θ_1 is the angle between the tangent to the surface and the freestream direction, and C_{pmax} is given in terms of γ and the freestream Mach number (M_1) as

22

$$C_{p_{max}} = \frac{2}{\gamma M_1^2} \left(\left[\frac{(\gamma+1)^2 M_1^2}{4\gamma M_1^2 - 2(\gamma-1)} \right]^{\frac{\gamma}{\gamma-1}} \left[\frac{1-\gamma+2\gamma M_1^2}{\gamma+1} \right] - 1 \right) \quad (20)$$

Defining ϕ as the angle between the normal to the surface and the freestream, then equation 19 can be written as

$$C_p = C_{p_{max}} \cos^2 \phi \quad (21)$$

Defining C_p as

$$C_p = \frac{p_e - p_1}{q_1} \quad (22)$$

where the subscript 1 denotes the freestream condition, then equation 21 can be written as:

$$\frac{p_e - p_1}{q_1} = C_{p_{max}} \cos^2 \phi \quad (23)$$

where q_1 is the dynamic pressure of the freestream. Equation 23 can be written as

$$p_e = C_{p_{max}} q_1 \cos^2 \phi + p_1 \quad (24)$$

Differentiating equation 24 with respect to x, we obtain

$$\frac{dp_e}{dx} = -2 C_{p_{max}} q_1 \cos\phi \sin\phi \frac{d\phi}{dx} \quad (25)$$

Substituting equation 25 into equation 18, we have

$$\frac{du_e}{dx} = \frac{2 C_{p_{max}} q_1}{\rho_e u_e} \cos\phi \sin\phi \frac{d\phi}{dx} \quad (26)$$

Consider the stagnation region, as shown in Figure 7.

23
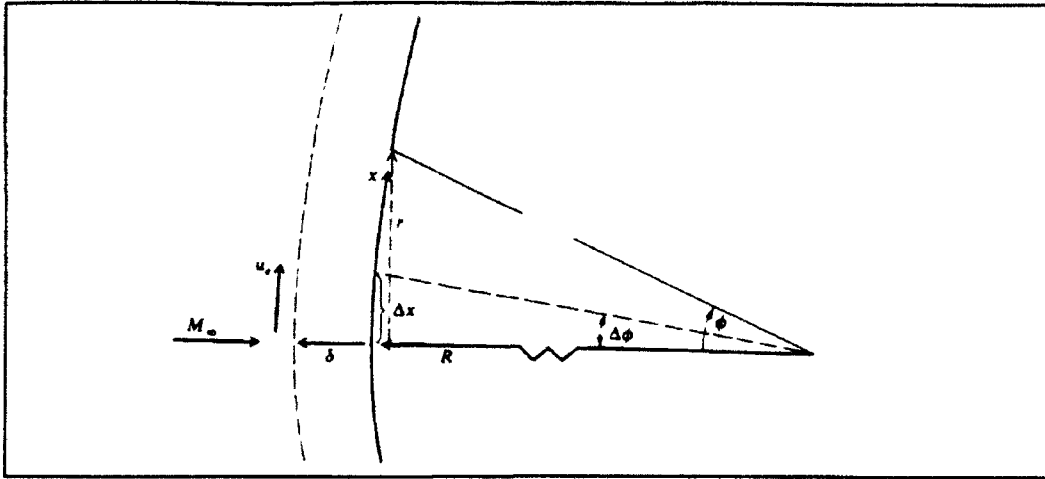
Figure 7: Stagnation Region of a Blunt Body [Ref.5:p. 251].

In this region, let Δx be a small increment of surface distance above the stagnation point, corresponding to small changes in ϕ of $\Delta\phi$. Since the flow velocity is so low in the stagnation region, we can assume [Ref. 5:p. 252]

$$u_e = (\frac{du_e}{dx})_s \Delta x \qquad (27)$$

In the stagnation region the following approximations can be made if ϕ is small:

$$\cos\phi \approx 1 \qquad (28a)$$

$$\sin\phi \approx \phi \approx \Delta\phi \approx \frac{\Delta x}{R} \qquad (28b)$$

$$\frac{d\phi}{dx} = \frac{1}{R} \qquad (28c)$$

where R is the radius of the nose of the body at the stagnation point.

With the approximation of equation 28a and substituting into equation 22, equation 21 becomes

$$C_p = C_{P_{max}} = \frac{p_e - p_1}{q_1} \qquad (29)$$

which is rewritten as

$$q_1 = \frac{1}{C_{P_{max}}} (p_e - p_1) \qquad (30)$$

Substituting equations 27-30 into equation 26 and rearranging terms gives

$$\frac{du_e}{dx} = \frac{1}{R} \sqrt{\frac{2(p_e - p_1)}{\rho_e}} \qquad (31)$$

This value for the velocity gradient is then substituted into the value for V in equation 17.

The velocity, temperature, density, Mach number, and pressure immediately behind the shock wave can be determined from the normal and oblique shock relations contained in Anderson [Ref. 2:pp.67-68,106]. The density behind the shock along the stagnation streamline is used in equation 17 for the value of ρ.

Equation 17 gives the boundary layer thickness at the stagnation point of a two dimensional body. The boundary layer thickness for an axisymmetric body will be thinner than for the two dimensional case [Ref. 5:p. 254]. While the difference between the axisymmetric and two dimensional cases is noted, equation 17 does provide an

25

approximation of the boundary layer thickness for the
axisymmetric case at the stagnation point.

b. Boundary Layer Edge Conditions

The pressure distribution at the surface of the
body is approximated by the modified newtonian method [Ref.
5:pp. 53-56]. Although the results provided by this method
are not very accurate at low supersonic Mach numbers, the
results improve quickly as Mach number increases [Ref.5:pp.
45-56]. The pressure coefficient at the surface of the body
using the modified newtonian method is given by equation 19.
Recalling from equation 22 the definition for C_p, the
pressure at the boundary layer edge over the nose of the
body is approximated by

$$p_e = C_{p_{max}} q_1 \cos^2\theta + p_1 \tag{32}$$

Figure 8 shows the surface pressure distribution over the
nose of the hypothetical vehicle used in this analysis for
selected Mach numbers. The nose radius (R) in Figure 8 is
1.5 ft (.4572 m) and the pressure distribution is shown from
the stagnation point through an angle of 68.2 degrees, where
the rounded nose intersects the cone of the body.

The total temperature behind the shock wave
remains constant everywhere behind the shock. Also, we
assume that the total pressure is constant along the
streamline that enters through the nearly normal portion of
the shock and flows along the boundary layer edge. These

26

values can be calculated and used as a reference to obtain local values of temperature and pressure.
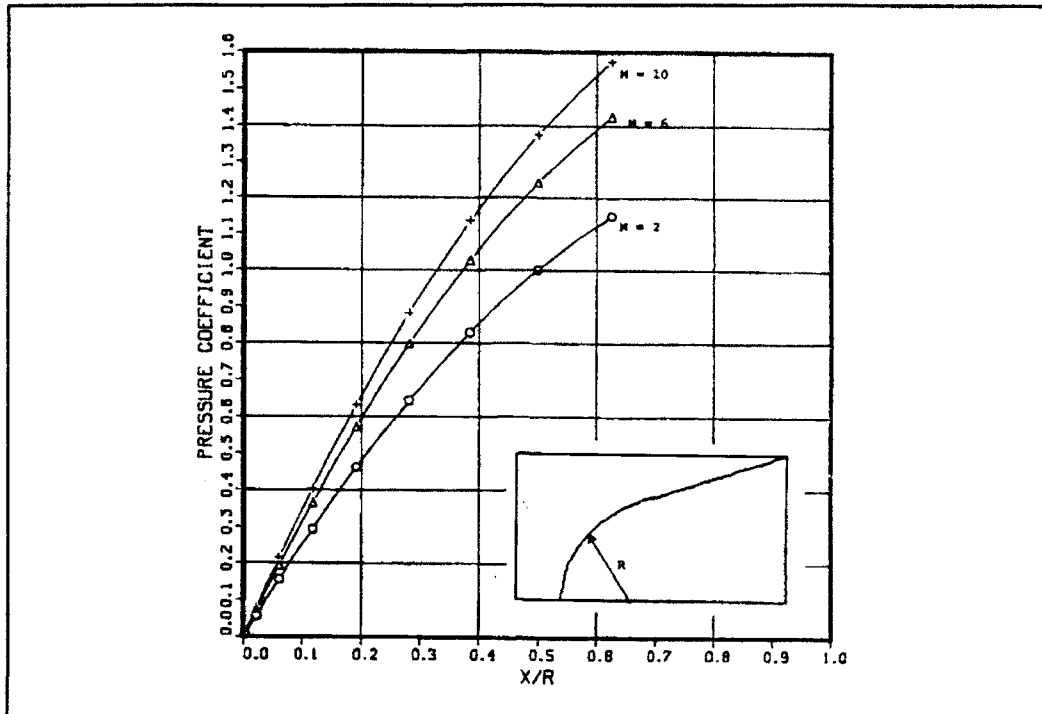
Figure 8: Pressure Distribution Over a Blunt Nose Cylindrical Cone Body.

The total pressure in the freestream is given by

$$P_{0_1} = P[(1 + \frac{\gamma-1}{2} M_1^2)^{\frac{\gamma}{\gamma-1}}] \qquad (33)$$

where P_{01} is the stagnation pressure in the freestream, P is the static pressure of the freestream. For these analyzes all freestream atmospheric conditions were taken from Reference [6] at an altitude of 30,000 meters. The ratio of stagnation pressures across the shock is

27

$$\frac{P_{0_2}}{P_{0_1}} = e^{-\frac{s_2 - s_1}{R'}} \tag{34}$$

where R' is the specific gas constant, and s_2-s_1 is given by

$$s_2 - s_1 = c_p \ln\left[\left(1 + \frac{2\gamma}{\gamma + 1}(M_1^2 - 1)\right)\left(\frac{2 + (\gamma - 1)M_1^2}{(\gamma + 1)M_1^2}\right)\right] \tag{35}$$
$$- R\ln\left[1 + \frac{2\gamma}{\gamma + 1}(M_1^2 - 1)\right]$$

where c_p is the specific heat at constant pressure of the gas. The stagnation pressure behind the shock is then obtained by taking the product of equations 33 and 34

$$P_{0_2} = \left(\frac{P_{0_2}}{P_{0_1}}\right)P_{0_1} \tag{36}$$

The stagnation temperature in the freestream is calculated by

$$T_{0_1} = T\left(1 + \frac{\gamma - 1}{2}M_1^2\right) \tag{37}$$

where T is the freestream temperature. The total temperature across a normal shock is constant, therefore

$$T_{0_1} = T_{0_2} \tag{38}$$

If we substitute T_{02} for T_{01} in equation 37, and with a known Mach number, the local temperature can be determined.

The sonic point on the body nose is located with the same method used in determining the shock shape, and is described in Appendix A. Since the Mach number at the sonic

28

line is one, the local pressure at the sonic point can be obtained by substituting the value of P_{02}, from equation 36, for P_{01} in equation 33. Once the sonic point is located, the angle between the body centerline and the sonic point can be easily calculated. This angle will be designated the sonic point angle (SPA) for calculation purposes. The total angle that the flow makes as it rounds the nose is 68.2 degrees. Subtracting the SPA from 68.2 gives the remaining angle, designated A_1, that the flow must turn through in traveling from the sonic line to the cone portion of the body. Treating angle A_1 as a Prandtl-Meyer expansion angle, the pressure, Mach number, and temperature of the flow downstream of the expansion can be calculated.

Before proceeding further, it is necessary to introduce the Prandtl-Meyer function [Ref. 2:p. 134], which is given the symbol ν

$$\nu(M) = \sqrt{\frac{\gamma+1}{\gamma-1}} \tan^{-1} \sqrt{\frac{\gamma-1}{\gamma+1}(M^2-1)} - \tan^{-1}\sqrt{M^2-1} \qquad (39)$$

As can be seen from equation 39, the Prandtl-Meyer function is a function of the Mach number and γ. Let $\nu(M_1)$ be the Prandtl-Meyer function before the expansion, and $\nu(M_2)$ be the Prandtl-Meyer function after the expansion. Then the angle A_1 that the flow turns through is

29

$$A_1 = \nu(M_2) - \nu(M_1) \qquad\qquad (40)$$

At the sonic line the Mach number is one, and therefore $\nu(M_1)$ in equation 40 is zero and $A_1 \cdot \nu(M_2)$. Putting the known value of A_1 into equation 39 for $\nu(M)$, the Mach number after the expansion can be determined. This process is repeated at the point where the cone joins the body. In this fashion the flow Mach number along the length of the cylindrical portion of the vehicle can be found. With the Mach number known and the previously calculated values of total pressure and total temperature, the local pressure and temperature along the cylindrical portion of the body can be determined using equations 33 and 37. These values will be taken as the conditions at the edge of the boundary layer.

c. Boundary Layer Thickness

The boundary layer is formed as a result of the no slip condition that exists at the wall of a body immersed in a flow (see Figure 6). As the flow progresses along the length of the body, the thickness (δ) of the layer of retarded flow increases as more and more fluid becomes affected [Ref. 14:p. 25]. The thickness of the boundary layer on a flat plate at zero incidence can be calculated using the method developed by Blasius [Ref. 16]. For laminar flow the boundary layer thickness was found to be

$$\delta \approx \frac{5x}{\sqrt{Re_x}} \qquad\qquad (41)$$

where x is the distance along the plate, and Re_x is the Reynolds number (see equation 12) as a function of distance along the plate. For a turbulent boundary layer the thickness is given by [Ref. 12:p. 13]

$$\delta \simeq \frac{0.37x}{(Re_x)^{1/5}} \qquad (42)$$

As previously stated, the boundary layer on an axisymmetric body is thinner than on a flat plate. However, as a first approximation, the boundary layer over a flat plate with a length equal to the distance traveled by the flow from the stagnation point to the tail end of the body will be used to approximate the boundary layer thickness. This approximation is reasonable when $\delta << R$ as it is in this case.

Since there is a dramatic difference in the growth of laminar vs turbulent boundary layers, it is necessary to establish the point where transition occurs. In actuality transition may occur over a finite distance making prediction of a point of transition extremely difficult. Research to determine exactly how transition occurs and methods to predict its occurrence are ongoing. A formula developed by Anderson [Ref. 5:p 280] to predict the point of transition will be used in this analysis.

$$\log_{10}(Re_T) = 6.421\exp[1.209\times10^{-4}M_e^{2.641})\qquad\textbf{(43)}$$

where Re_T is the Reynolds number at which transition occurs, and M_e is the Mach number at the boundary layer edge. It should be recognized that the data used to develop this equation was unknown to the author and that equation 42 was being used as an approximation.

B. BASE PRESSURE DETERMINATION

If the assumption is made that the launch vehicle is a projectile with no exhaust plume, the pressure behind the body in the wake is assumed to be the freestream static pressure. This assumption is supported by Anderson [Ref. 5:pp 117-138] who shows that for a cylindrical body with fineness ratio greater than six, the pressure asymptotically approaches freestream pressure. The assumption of no exhaust plume allows calculation of the entropy change as a result of the boundary layer on the body, but ignores the effects of boundary layer/plume interaction.

With the pressure in the wake being approximately equal to static pressure and the stagnation pressure behind the shock, from equation 36, the Mach number in the wake can be determined using equation 33. The difference between the Mach number in the wake and in the flowfield can be used to calculate the difference between the velocities (U-u) needed to solve equation 6. These values are summarized in Table 3.

C. WAKE PROFILE

The wake boundary is established from the body plus the boundary layer thickness at the base of the body. Traveling downstream for several body diameters and assuming the same rate of growth of the boundary layer, the distance from the centerline to the point where the wake velocity approaches the freestream velocity can be determined. This is shown in Figure 9. For calculation purposes, a distance of five diameters downstream of the base was arbitrarily chosen.

TABLE 3: COMPARISON OF FREESTREAM AND WAKE MACH NUMBER

Freestream Mach (M_f)	Wake Mach (M_w)	M_w/M_f
1.1	1.0991	.9992
2.0	1.7879	.8939
3.0	2.2769	.7590
4.0	2.6351	.6588
5.0	2.9218	.5844
6.0	3.1630	.5272
7.0	3.3725	.4818
8.0	3.5586	.4448
9.0	3.7265	.4141
10.0	3.8800	.3880
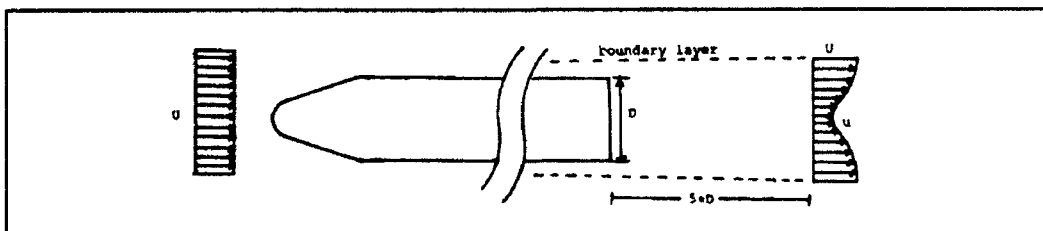
Figure 9: Illustration of Wake Profile.

The variation of u in the wake from the centerline to the point where u≈U is given by

$$u = U_w + x(1 - \frac{U_w}{U_1}) U_1 \qquad (44)$$

where U_w is the minimum wake velocity, U_1 is the freestream velocity, and x is a scaling variable where 0≤x≤1. The distance from the centerline to the point where u≈U is given by

$$y = (R_b + \delta_t) \pi \qquad (45)$$

where R_b is the radius of the base of the body and δ_t is the thickness of the boundary layer extended to the point in the wake where the profile is being calculated.

D. DRAG DETERMINATION

The drag of the body is calculated using equation 6 which is repeated here:

$$D = \int_A \rho u (U - u) \, dA \qquad (46)$$

Since the velocity in the wake varies along the centerline, designated the x axis, and with the distance from the centerline, designated the y axis, equation 46 becomes the following double integral:

$$D = \int_0^y \int_0^1 2 \pi r \rho u (U - u) \, dr \qquad (47)$$

where u and y are given by equations 44, and 45 respectively. The density in equation 47 is the density at

34

the location in the wake where the profile is determined.
For these calculations this value was approximated using the
perfect gas equation. The pressure is taken as freestream
and the temperature is that calculated for the boundary
layer temperature just forward of the base of the body
ignoring plume effects.

E. ENTROPY CALCULATION

With the drag determined, the entropy flux increase as a
result of the boundary layer can now be calculated using
equation 11 which is repeated here

$$DU = T_1 \frac{S}{\sec} \tag{48}$$

where U and T_1 are the freestream velocity and temperature
respectively, and D is the drag.

For the body shape used in this analysis and with the
approximations used to calculate the required flowfield
parameters, the entropy increase is presented in Table 4.

As can be seen from Table 4, the entropy increase in the
boundary layer starts to decrease above M=7. This occurs due
to the boundary layer becoming thinner at higher Ma h
numbers. The thinner boundary layer is a result of the
transition point moving aft on the body. Initially the
transition point moves forward toward the nose of the body.
Between 6≤M≤7, the transition point stops moving toward the
nose and starts moving back toward the tail. This is
occurring as a result of the laminar to turbulent

35

TABLE 4: ENTROPY INCREASE DUE TO THE BOUNDARY LAYER

Mach number	Rate of Entropy Increase (KJ/sec)
1.1	2918
2	21230
3	48316
4	70635
5	84925
6	92074
7	92671
8	87442
9	77123
10	62372

transition point as calculated by equation 43. The
transition Reynolds number increases exponentially with
increasing Mach number. For a given transition Reynolds
number, the point of transition is obtained by substituting
Re_T for Re and x for l in equation 12, and rearranging

$$x = \frac{Re_T\mu}{\rho V} \tag{49}$$

As Re_T increases exponentially, the numerator in equation 49
grows faster than the denominator, as shown in Figure 10.
The result of this is that the transition point moves toward
the tail of the body and the boundary layer remains laminar
longer. Since entropy is produced at a higher rate in
turbulent boundary layers, the net result is that less
entropy production occurs.

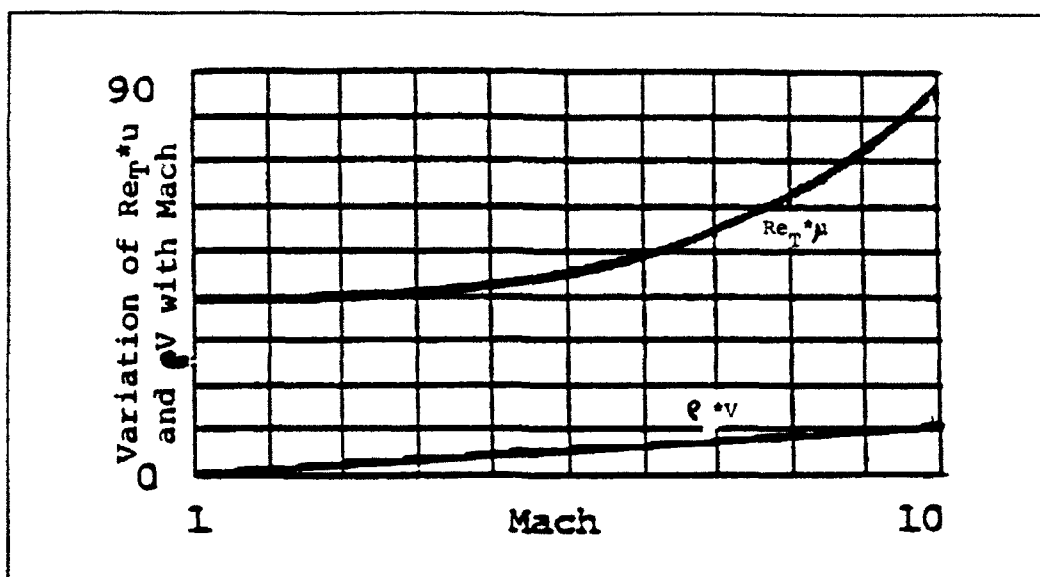**Figure 10: Variation of Transition Point Parameters With Mach Number.**

This phenomenon is a result of using equation 43 to predict the transition point and may not be an accurate representation of actual flow. As previously stated, the data that equation 43 was developed from was unknown to the author, and the conditions of this study may be outside the range for which equation 43 is valid.

IV. CONCLUSIONS

Recall from the exergy equation (equation 1) that an increase in entropy results in a corresponding decrease in exergy. A primary advantage of exergy analysis is the identification of those processes or areas that have the highest exergy loss and hence the greatest potential for improved efficiency. A method to quantify the exergy decrease resulting from entropy production across the shock wave and in the boundary layer, ignoring high temperature effects, has been presented.

It has been demonstrated that the exergy decrease due to the production of entropy across the shock wave and in the boundary layer can be calculated for a typical space launch vehicle. This information can be used to highlight those areas which have the greatest potential for improved efficiency.

For the conditions of this study and within the accuracy of the approximations, it is clearly evident that entropy production is much greater in the boundary layer than across the shock wave for a given Mach number. This indicates that, all other factors being equal, design efforts should concentrate on reducing the entropy production in the boundary layer.

V. RECOMMENDATIONS FOR FURTHER RESEARCH

This thesis applies the method of exergy analysis to two areas of interest for space launch vehicles. In doing so, it provides an initial step in the development of an exergy methodology tool for design purposes.

Following the work of Czysz [Ref. 21], application of this methodology to launch vehicle propulsion systems would be beneficial.

Alternately, variations in launch vehicle design could be examined with the goal of finding the optimum design to minimize entropy production across the shock wave and within the boundary layer.

It would also be useful to determine the magnitude of the error for the approximations used in this study. This could be accomplished by comparing the results with those obtained from exact flowfield calculations using CFD methods. Also the effects of the boundary layer/plume interactions on entropy production could be investigated.

APPENDIX A
THE SHOCK WAVE MODEL

This program computes the entropy increase across the shock wave of a cylindrical space launch vehicle with a blunt cone nose. The program is written for Mach numbers of 1.1 to 10, and for atmospheric conditions at an altitude of 30,000 meters. This program is written in Fortran 77 code. Comment statements are preceded by a "C".

```
C     Variable declarations

C     M = Freestream Mach number
C     BETA = Cotangent of the Mach number
C     THETA = The shock wave angle for sonic flow behind the
C           shock
C     DELTA = The maximum stream deflection angle that can
C           occur without shock separation
C     NU = Angle between the sonic line and a line normal to
C           the freestream direction
C     GAMMA = Ration of specific heats (1.4 for air)
C     SIGMA = Angle of shock wave at the center of mass
C           streamline
C     A = Area ratio for isentropic flow
C     P = Stagnation pressure ratio
C     RATIO = Ratio of the distance from the x-axis to the
C           shock sonic point to the distance from the x-axis
C           to the body sonic point
C     YSB = Distance from the centerline of the body to the
C           sonic point on the body
C     X0 = Distance from foremost point of detached shock to
C           intercept of its asymptote on the x-axis
C     Y = Coordinate perpendicular to freestream flow
C     X = Coordinate in the direction of the freestream
C     I,J,Z = Increment counters
C     PI = Radian equivalent of 180 degrees
C     DIFF = The difference between the shock wave angle and
C           the asymptote angle of the hyperbola that is
C           defined by the shock wave
C     CANGLE = The constant angle between the asymptote of
C           the hyperbola and the freestream direction
```

```
C      SANGLE = The angle between the freestream direction and
C             the tangent to the shock wave
C      ANGLED = The same angle as "SANGLE" but in degrees
C             instead of radians
C      TOTALS = The total change in entropy across the shock
C             wave

       START PROGRAM
       INTEGER I, J, Z
       PARAMETER (Z=10)
       REAL M(Z), BETA(Z), THETA(Z), DELTA(Z),
     +        NU(Z), PI, YSB(Z), SIGMA(Z), A(Z), P(Z),
     +      RATIO(Z), X0(Z), X(7500), Y(7500), DIFF, B(Z),
     +      CANGLE(Z), SANGLE(7500), ANGLED(7500), TOTALS
       PI=3.14159
       M(1)=1.1
       M(2)=2
       BETA(1)=SQRT(M(1)**2.0-1.0)
       BETA(2)=SQRT(M(2)**2.0-1.0)
       DO 05 I=3,Z
             M(I)=M(I-1)+1.0
             BETA(I)=SQRT(M(I)**2.0-1.0)
   05  CONTINUE
       CALL SHOCK(Z,M,THETA)
       CALL MAX(Z,M,DELTA)
       CALL AVG(Z,M,NU)
       CALL DISYSB(Z,DELTA,YSB)
       CALL CENTER(Z,THETA,BETA,SIGMA)
       CALL AREA(Z,M,A)
       CALL PRESS(Z,SIGMA,M,P)
       CALL SPRATIO(Z,P,A,NU,RATIO)
       CALL DISXO(Z,YSB,BETA,RATIO,THETA,X0)
C      The following do loop, for each Mach number, calculates
C      the angle of the asymptote of the hyperbola that
C      defines the shock. Then the point on the x and y
C      axis where the difference between the shock wave
C      angle and the asymptote angle is less than 1 per
C      cent is found. This defines the limit of the shock wave
C      for purposes of calculating the entropy change across
C      the shock. The change in entropy is then calculated.
       DO 15 J=1,Z
             B(J)=X0(J)/BETA(J)
             CANGLE(J)=ATAN(B(J)/X0(J))
             CALL SHAPE(X0(J),BETA(J),X,Y,)
             CALL SWANGLE(X0(J),BETA(J),Y,SANGLE,ANGLED)
                  DO 10 I=2,7500
                  IF (SANGLE(I).EQ.0) GO TO 10
                  DIFF=(SANGLE(I)-CANGLE(J))/CANGLE(J)
                  IF(DIFF.GT.0.01) GO TO 10
                  IF(DIFF.LE.0.01) THEN
                  CALL TOTAL(M(J),X0(J),BETA(J),X(I),TOTALS)
                  GO TO 15
```

41

```
                    END IF
     10  CONTINUE
     15  CONTINUE
         STOP
         END


C        Calculate the shock wave angle for sonic flow behind
C        the shock
         INTEGER I,Z
         REAL M(Z), THETA(Z), GAMMA
         GAMMA=1.4
         DO 05 I=1,Z
                THETA(I)=ASIN(SQRT((1.0/4.0*GAMMA*M(I)**2.0))
     +          *((GAMMA+1.0)*M(I)**2.0-(3.0- GAMMA)
     +          +(SQRT((GAMMA+1.0)*((GAMMA+1.0)*M(I)**4.0-2.0
     +          *(3.0-GAMMA)*M(I)**2.0+(GAMMA+9.0))))))))
     05  CONTINUE
         RETURN
         END


C        Calculate the maximum deflection angle, in radians,
C        for a given freestream Mach number in air. For this
C        calculation, the maximum deflection angle without shock
C        detachment was calculated from NACA report 1135, chart
C        5. An equation for the line of maximum deflection was
C        obtained by performing a curve fit of the data
C        presented in the chart.
         SUBROUTINE MAX(Z,M,DELTA)
C        NLOG = Natural log of Mach number between 1.1 and 10
C        TVAR = Natural log of shock wave detachment angle in
C               degrees
         INTEGER I,Z
         REAL M(Z), NLOG(10), TVAR(10), DELTA(Z)
         DO 05 I=1,Z
                NLOG(I)= LOG(M(I))
                TVAR(I)=3.80568+0.41631*LOG(NLOG(I))
                DELTA(I)=(EXP(TVAR(I)))/57.29578
     05  CONTINUE
         RETURN
         END


C        Calculate the angle between the sonic line and a line
C        normal to the freestream direction
         SUBROUTINE AVG(Z,M,NU)
         INTEGER I,Z
         REAL M(Z), NU(Z)
         DO 05 I=1,Z
                NU(I)=(3.9901+56.9298*LOG(M(I)))/57.29578
     05  CONTINUE
         RETURN
```

```
      END

C     Calculate the distance from the body centerline to the
C     sonic point on the body
      SUBROUTINE DISYSB(Z,DELTA,YSB)
C     DIST1=Distance along a line drawn tangent to the body
C           sonic point from the x-axis to the sonic point on
C           the body
C     R=Radius of the body apex (in feet)
C     ANG3=The angle between the x-axis and a line
C           perpendicular to DIST1 at the body sonic point and
C           extending from the sonic point to the x-axis
      INTEGER I,Z
      REAL PI, YSB(Z), DIST1(10), R, ANG3(10), DELTA(Z)
      PI=3.14159
      R=1.5
      DO 05 I=1,Z
           ANG3(I)=PI-(PI/2.0)-DELTA(I)
           DIST1(I)=R*((SIN(ANG(I))/SIN(DELTA(I))))
           YSB(I)=DIST1(I)*SIN(DELTA(I))
   05 CONTINUE
      RETURN
      END


C     Calculate the angle of the shock wave at the center
C     of mass streamline between the shock wave vertex
C     and the sonic point of the shock wave
      SUBROUTINE CENTER(Z,THETA,BETA,SIGMA)
      INTEGER I, Z
      REAL THETA(Z), BETA(Z), SIGMA(Z)
      DO 05 I=1,Z
           SIGMA(I)=ATAN(((TAN(THETA(I)))**2.0*(3.0/2.0)**2.0
     +     -(1.0/BETA(I))**2.0)*((3.0/2.0)**2.0-1.0))**0.5)
   05 CONTINUE
      RETURN
      END


C     Calculate the area ratio for isentropic flow
      SUBROUTINE AREA(Z,M,A)
      INTEGER I,Z
      REAL GAMMA, M(Z), A(Z)
      GAMMA=1.4
      DO 05 I=1,Z
           A(I)=((GAMMA+1.0)/2.0)**((GAMMA+1.0)/(2.0
     +     *GAMMA-1.0)))*M(I)*(1.0+((GAMMA-1.0)/2.0)
     +     *M(I)**2.0)**(-((GAMMA+1.0)/(2.0*(GAMMA-1.0))))
   05 CONTINUE
      RETURN
      END
```

```
C      Calculate the ratio between stagnation pressure before
C      and after the shock wave for a given shock wave angle
       SUBROUTINE PRESS(Z,SIGMA,M,P)
       INTEGER I, Z
       REAL GAMMA, SIGMA(Z), M(Z), P(Z)
       GAMMA = 1.4
       DO 05 I=1,Z
            PI(I)=1.0/((((GAMMA+1.0)*M(I)**2.0*
     +      SIN(SIGMA(I))**2.0)/((GAMMA-1.0)*
     +      M(I)**2.0*SIN(SIGMA(I))**2.0+2.0))**(GAMMA/
     +      (GAMMA-1.0))*((GAMMA+1.0)/(2.0*GAMMA*M(I)**2.0*
     +      SIN(SIGMA(I))**2.0-(GAMMA-1.0)))**
     +      (1.0/(GAMMA-1.0)))
   05 CONTINUE
       RETURN
       END


C      Calculate the ratio of the distance from the x-axis to
C      the shock sonic point to the distance from the x-
C      axis to the body sonic point
       SUBROUTINE SPRATIO(Z,P,A,NU,RATIO)
       INTEGER I,Z
       REAL P(Z), A(Z), NU(Z), RATIO
       DO 05 I=1,Z
            RATIO(I)= 1.0/((1.0-P(I)*A(I)*COS(NU(I)))**0.5)
   05 CONTINUE
       RETURN
       END


C      Calculate the distance from the foremost point of the
C      detached shock wave to the intercept of its asymptote
C      on the x-axis
       SUBROUTINE DISX0(Z,YSB,BETA,RATIO,THETA,X0)
       INTEGER I, Z
       REAL YSB(Z), BETA(Z), RATIO(Z), THETA(Z), X0(Z)
       DO 05 I=1,Z
            X0(I)=YSB(I)*BETA(I)*RATIO(I)*((BETA(I))**2.0*
     +      (TAN(THETA(I)))**2.0-1.0)**0.5
   05 CONTINUE
       RETURN
       END


C      Calculate the x and y coordinates for any point on the
C      shock wave
       SUBROUTINE SHAPE(X0,BETA,X,Y)
       INTEGER I
       REAL X(7500), Y(7500), BETA, X0
       X(1)=0.1
       Y(1)=0
       DO 05 I=2,7500
            X(I)=X(I-1)+0.2
            IF(X(I).LT.X0) THEN
```

44

```
            Y(I)=0
            ELSEIF (X(I).GE.X0) THEN
            Y(I)=SQRT(X(I)**2.0-X0**2.0)/BETA
            END IF
   05 CONTINUE
      RETURN
      END


C     Calculate the angle between the freestream and a line
C     drawn tangent to the shock wave at any point
      SUBROUTINE SWANGLE(X0,BETA,Y,SANGLE,ANGLED)
      INTEGER I
      REAL X0, BETA, Y(7500), SANGLE(7500), PI, ANGLED(7500)
      PI=3.14159
      DO 05 I=1,7500
            IF (Y(I).EQ.0) THEN
            SANGLE(I)=0
            ELSEIF (Y(I).GT.0) THEN
            SANGLE(I)=ATAN((SQRT(X0**2.0+BETA**2.C*Y(I)**2.0))
     +      /(BETA**2.0*Y(I)))
            ANGLED(I)=SANGLE(I)*180/PI
            END IF
   05 CONTINUE
      RETURN
      END


C     Calculate the total change in entropy across the shock
C     wave. All calculations are in SI units
C     RO=The density of air. For these calculations this
C           value is taken from the ICAO standard atmosphere
C           tables at an altitude of 30,000 meters.
C     TEMP=The temperature in degrees Kelvin of the
C           atmosphere at 30,000 meters altitude, taken from
C           the ICAO standard atmosphere tables
C     GAMMA=Ratio of specific heats
C     SGC=Specific gas constant. Assuming an ideal gas, for
C           air this value is 287 Joules/Kg-K
C     SSA=Local speed of sound in air
C     VEL=Velocity, in meters per second, of the freestream
C     SHCV=Specific heat of air at constant volume
C     PI=Radian equivalent of 180 degrees
C     LLINT=Lower limit of integration. The starting point,
C           located at the shock wave vertex, for numerical
C           integration to calculate the entropy change across
C           the shock wave
C     ULINT=Upper limit of integration. The ending point for
C           numerical integration across the shock wave
C     H=The integration step size for application of
C           Simpson's rule
C     N=The number of Simpson's rule integrations, and the
C           ending point for summation of individual
C           integrations
```

```
C      CENTERX=The center point, along the x-axis, for each
C           Simpson's rule integration
C      TSTEP=Specifies the beginning (TSTEP(1)), center
C           (TSTEP(2)), and end (TSTEP(3)) points for
C           Simpson's rule application for each individual
C           summation
C      RADIUS=The distance from the centerline x-axis to the
C           shock wave at each TSTEP location
C      TANGLE=The shock wave angle at each point of
C           intersection of the radius and the shock wave
C      DELTAE=Change in entropy per mass flow across the shock
C           at each point of intersection of RADIUS with the
C           shock wave
C      DELTAS=Distance along the shock at each interval of
C            integration
C      HOLD=Temporary storage variable
       INTEGER I, K
       REAL X0, X, BETA, DELTAE(3), TOTALS, LLINT, ULINT, H,
     +      CENTERX, PI, RADIUS(3), SHCV, GAMMA, TANGLE(3),
     +      TSTEP(3), RO, VEL, SSA, TEMP, M, DELTAS
       RO=.01841
       TEMP=226.509
       GAMMA=1.4
       SGC=287
       SSA=SQRT(GAMMA*SGC*TEMP)
       VEL=M*SSA
       SHCV=717.5
       PI=3.14159
       LLINT=X0*.3048
       ULINT=X*.3048
       HOLD=0
       H=0.5
       N=INT((ULINT-LLINT)/(2.0*H))
       CENTERX=LLINT+.05
       DO 05 I=LLINT, N
            DO 10 K=1,3
            TSTEP(1)=CENTERX-.05
            TSTEP(2)=CENTERX
            TSTEP(3)=CENTERX+.05
            IF (TSTEP(K).LE.LLINT) THEN
            RADIUS(K)=0
            TANGLE(K)=0
            DELTAE(K)=0
            GO TO 10
            END IF
       RADIUS(K)=(SQRT(TSTEP(K)**2.0-LLINT**2.0))/BETA
       TANGLE(K)=ATAN((SQRT(LLINT**2.0+BETA**2.0*RADIUS(K)
     +      **2.0))/(BETA**2.0*RADIUS(K)))
       DELTAE(K)=SHCV*(LOG((2.0*GAMMA*M**2.0*SIN(TANGLE(K))
     +      **2.0-(GAMMA-1.0))/(GAMMA+1.0))-GAMMA*
     +      LOG(((GAMMA+1.0)*M**2.0*SIN(TANGLE(K))**2.0)/
     +      ((GAMMA-1.0)*M**2.0*SIN(TANGLE(K))**2.0+2.0)))
```

```
10 CONTINUE
   DELTAS=(0.1*.3048)/COS(TANGLE(2))
   HOLD=HOLD+(((H/3.0)*(DELTAE(1)+4.0*DELTAE(2)
  +      +DELTAE(3)))*RO*2.0*PI*RADIUS(2)*DELTAS*VEL*
  +      SIN(TANGLE(2)))
   CENTERX=CENTERX+0.1
05 CONTINUE
   TOTALS=HOLD*TEMP
   RETURN
   END
```

LIST OF REFERENCES

1. Ahern, J.E., *The Exergy Method of Energy Systems Analysis*, John Wiley and Sons, 1980.

2. Anderson, J.D., *Modern Compressible Flow With Historical Perspective*, McGraw Hill Book Co., 1990.

3. National Advisory Committee for Aeronautics Technical Note 1921, *Approximate Method for Predicting Form and Location of Detached Shock Waves Ahead of Plane of Axially Symmetric Bodies*, by W.E. Moeckel, 1949.

4. National Advisory Committee for Aeronautics Technical Note 4170, *A Reexamination of the Use of Simple Concepts for Predicting the Shape and Location of Detached Shock Waves*, by E.S. Love, December 1957.

5. Anderson, J.D., *Hypersonic and High Temperature Gas Dynamics*, McGraw Hill Book Co., 1989.

6. International Civil Aviation Organization, *Standard Atmosphere Manual*, Government Printing Office, Washington, DC, 1964.

7. National Advisory Committee for Aeronautics Report 1135, *Equations, tables, and Charts for Compressible Flow*, by Ames Research Staff, 1953.

8. Sears, W.R., *General Theory of High Speed Aerodynamics*, Princeton University Press, 1954.

9. Crocco, L., *Eine neue Stromfunktion fur die der Bewegung der Gase mit Rotation*, Z. Angew. Math. Mech. vol. 17, 1937, pp. 1-7.

10. Oswatitsch, K., *Der Luftwiderstand als Integral des Entropiestromes*, Nachr. Ges. Wiss. Gottingen. Math. Phys. Kl., 1945.

11. Prandtl, L., *Uber Flussigkeitsbewegung bei sehr Kleiner Reibung*, Proc III International Mathimatical Congress, Heidelberg, Germany, 1904.

12. Young, A.D., *Boundary Layer*, American Institute of Aeronautics and Astronautics, 1989.

13. Anderson, J.D., *Fundamentals of Aerodynamics*, McGraw Hill Book Co., 1984.

14. Schlichting, H., *Boundary Layer Theory*, 7th Ed., McGraw Hill Book Co., 1979.

15. Moran, J., *An Introduction to Theoretical and Computational Aerodynamics*, John Wiley and Sons, Inc., 1984.

16. National Advisory Committee for Aeronautics Technical Memorandum 1256, *The Boundary Layers in Fluids With Little Friction*, by H. Blasius, 1950.

17. von Karman, T., and Moore, N.B., *Resistance of Slender Bodies Moving With Supersonic Velocities With Special Reference to Projectiles*, A.S.M.E., Transactions, pp. 303-310, 1932.

18. National Advisory Committee for Aeronautics Technical Note 2137, *An Analysis of Base Pressure at Supersonic Velocities and Comparison With Experiment*, by D.R. Chapman, July 1950.

19. National Advisory Committee for Aeronautics Technical Note 3393, *An Experimental Investigation of the Base Pressure Characteristics of Non Lifting Bodies of Revolution at Mach Numbers from 2.73 to 4.98*, by J.O. Reller and F.M. Hanaker, March 1955.

20. Hoerner, S.F., *Fluid-Dynamic Drag*, Published by the Author, 1965.

21. Czysz, P., *Energy Analysis of Propulsion Systems for High Speed Vehicles*, 27th Aerospace Sciences Meeting, January 9-12, 1989.

INITIAL DISTRIBUTION LIST

		No. of Copies
1.	Defense Technical Information Center Cameron Station Alexandria, Virginia 22304-6145	2
2.	Library, Code 52 Naval Postgraduate School Monterey, California 93943-5002	2
3.	Professor Conrad F. Newberry, Code AA/NE Department of Aeronautics and Astronautics Naval Postgraduate School Monterey, California 93943-5100	6
4.	Commanding Officer Attn: LCDR Benjamin F. Roper, USN USS John Rodgers (DD-983) FPO AA 34092-1221	2